

# Mechanical pulping with a sequential velocity refiner — a new concept

CHARLES W. McMILLIN, U.S. Department of Agriculture, Southern Forest Experiment Station, Pineville, USA

Lecture given at the 1977 International Mechanical Pulping Conference in Helsinki, Finland

**KEYWORDS:** Mechanical pulping, Southern pines, Disk refiners, Design, Energy consumption, Chip groundwood, Fibers, Hand sheets, Mechanical properties.

**SUMMARY:** In previous research with refiner mechanical pulps, a theoretical stress analysis indicated that longitudinal tracheids of *Pinus taeda* L. fail while under torsional stress and unwind into ribbonlike elements that provide the coherence necessary for strength development. When macerated tracheids of loblolly pine were individually stressed in torsion and observed in a scanning electron microscope, the unwinding process was characterized by the formation of a crack, generally parallel to the zone of weakness delineated by the  $S_2$  layer fibril helix, followed by development of a ribbon with further twisting.

This principle of dynamic torsional unwinding has been applied to the design of a new type of double-disk refiner. Basically, the refiner consists of two counter-rotating surfaces, each composed of four concentric rings driven at sequentially increasing speeds. In theory, an individual intact fiber becomes radially aligned between the two disks where it then rotates in a clockwise direction about its longitudinal axis and is subjected to torsional stresses. As the rotating fiber moves in a radial direction between the disks, it passes the interface of two rings having increasing differential velocity. At this point, the upper end of the fiber (the end further along the disk radius) is suddenly forced to rotate at a substantially faster velocity than the lower end—a condition favoring higher levels of induced torsional stress and the desired unwinding.

Operating a laboratory version of this refiner with sequential velocity yielded higher quality pulp and stronger hand-sheets than operating it as a conventional double-disk refiner at equal energy input. Visual evaluation of the pulps revealed that fiber refined with sequential velocity contained fewer intact and more frazzled, broomed, and ribbon-strand particles than did fiber refined without sequential velocity.

□ Vid tidigare undersökningar av mekanisk massa ur flis visade en teoretisk analys att longitudinella trakeider av *Pinus taeda* L. brast under påverkan av torsionskrafter och avrullades som bandlelement, vilka åstadkom den erforderliga sammanhållningen för styrkeutveckling. Om enstaka söndermosade trakeider av loblolly-fur utsattes för torsion, visade elektronmikroskopi att avrullningsprocessen började med uppkomsten av en spricka, vanligen parallell med en svaghetszon utefter  $S_2$ -väggens fibrillspirale och som åtföljdes av bildandet av ett band vid fortsatt tvinnande.

Principen dynamisk avrullning under torsion har legat till grund för utformningen av en ny typ av raffinör med dubbla skivor. Raffinören består av två motroterande skivor, som vardera är sammansatta av fyra koncentriska ringar, vilka drivs med upptrappande hastigheter. Teoretiskt sett bör en enstaka opåverkad fiber lägga sig i radiell riktning mellan de två skivorna, där den roterar i högervarv omkring sin längdaxel och blir utsatt för torsionskrafter. Medan den roterande fibern förflyttar sig i radiell riktning mellan skivorna, passerar den gränsen mellan två ringar, av vilka den yttre löper med större hastighet. Därvid kommer den del av fibern som radiellt befinner sig längre ut att plötsligt tvingas till en kraftigt ökad rotationshastighet jämfört med dess andra del. Detta ger upphov till torsionsspänning och den önskade avrullningen.

Laboratorieraffinören med dessa upptrappande vinkelhastigheter ger högre massakvalitet och starkare bandark än när raffinören kördes konventionellt med samma energiförbrukning. Visuellt granskning gav vid handen att efter upp-trappande hastighet var färre fibrer orörda och mera uppslagna som band än vad som skedde utan sådan upp-trappning.

□ In früheren Untersuchungen mit Refiner-Holzstoffen deutete eine theoretische Belastungsanalyse darauf hin, dass Fasertracheiden von *Pinus taeda* L. während einer Torsionsbeanspruchung geschwächt werden und sich bändchenförmige Elemente abwickeln, die eine Kohärenz ermöglichen, die für

die Festigkeitsentwicklung notwendig ist. Werden macerierte Tracheiden von Loblolly Pine einzeln einer Torsionsbeanspruchung unterworfen und im Rasterelektronenmikroskop untersucht, so ist der Abwicklungsprozess durch das Auftreten eines Risses, meist parallel zur Schwächungszone, vorgezeichnet durch die Fibrillspirale der  $S_2$ -Schicht, charakterisiert, gefolgt von der Bildung eines Bändchens bei weiterer Verdrillung.

Das Prinzip dieses Abwickelmechanismus durch dynamische Verdrillung wurde zum Entwurf eines neuen Doppelscheiben-Refiners herangezogen. Im Prinzip besteht der Refiner aus zwei gegenläufigen Flächen, von denen jede aus vier konzentrischen Ringen besteht, die mit steigender Geschwindigkeit sich drehen. Theoretisch wird eine einzelne intakte Faser radial zwischen beiden Scheiben ausgerichtet und rotiert im Uhrzeigersinne um die Längsachse, wobei eine Torsionsbeanspruchung auftritt. Wenn die rotierende Faser in radialer Richtung zwischen den Scheiben sich fortbewegt, passiert sie die Übergangszonen zweier Ringe mit unterschiedlicher Geschwindigkeit. An dieser Stelle wird das „obere“ Faserende (welches, in radialer Richtung, sich weiter weg vom Zentrum befindet) plötzlich gezwungen merklich schneller zu rotieren als das „untere“ Ende — ein Zustand, der stärkere induzierte Torsionsbeanspruchungen hervorruft und damit die gewünschte Abwindung.

Der Betrieb einer Laboratoriumsausführung eines solchen Refiners mit stufenweisen Geschwindigkeiten lieferte einen Holzstoff von höherer Qualität, der festere Prüfblätter ergab als wenn der Refiner als konventioneller Scheibenrefiner bei gleicher Energieeinspeisung lief. Die visuelle Beurteilung des Holzstoffes zeigte, dass Fasern, die mit diesen stufenweisen Geschwindigkeiten raffiniert wurden, weniger intakte und mehr abgeriebene sowie ausgefranste Partikel und Bändchenbüschel bilden als solche Fasern, die ohne diesen stufenförmigen Antrieb gemahlen wurden.

**ADDRESS OF THE AUTHOR:** Southern Forest Experiment Station, Forest Service, U.S. Department of Agriculture, 2500 Shreveport Highway, Pineville, Louisiana 71360 USA.

In previous research on the process for making groundwood in a double-disk refiner (3), a theoretical stress analysis indicated that longitudinal tracheids of *Pinus taeda* L. may fail while under torsional stress and unwind into ribbonlike elements (*fig. 1*). Such elements provide the coherence necessary for strength development in mechanical pulps (2).

To verify the theory of dynamic torsional unwinding, macerated earlywood and latewood tracheids of loblolly pine were stressed in torsion with a specially designed fixture and observed at high magnification in a scanning electron microscope (4). Some tracheids buckled or sheared and yielded no ribbons, but the predominant failure was characterized by the formation of a crack followed by the fiber unwinding into a ribbon with further twisting.

The series of micrographs in *fig. 2* illustrate the formation of a ribbon in an earlywood fiber subjected to torsional stress applied in a clockwise direction. Micrograph A shows the undeformed fiber before application of stress. As the fiber is rotated, stresses in the cell wall increase. A critical point is eventually reached where the strength of the fiber is exceeded and a crack abruptly forms at the zone of weakness delineated by the  $S_2$  fibril helix (point 1 of micrograph B). After the initial crack, stresses in the tracheid are reduced, and additional

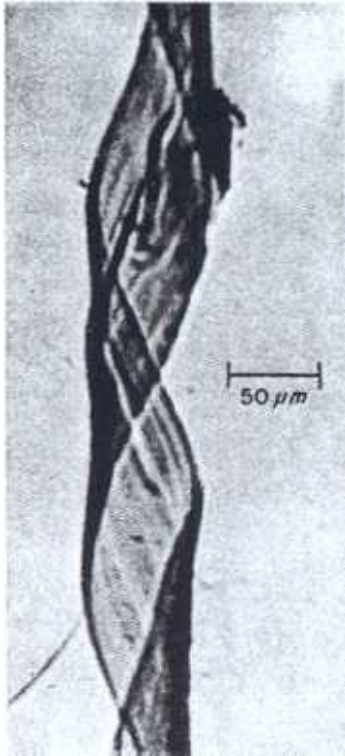


Fig. 1. Light micrograph of an unwound ribbon from a loblolly pine mechanical pulp.

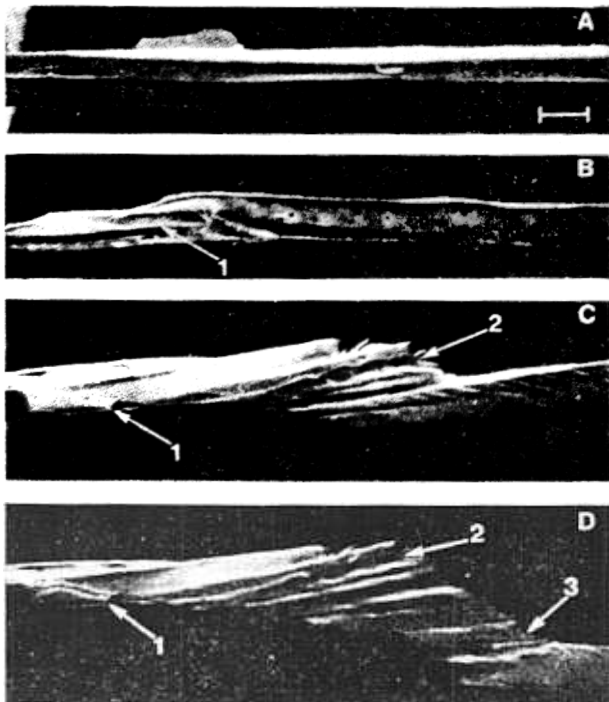


Fig. 2. Development of a ribbonlike particle in an earlywood tracheid of loblolly pine. The scale mark in A shows 50 μm and is also applicable to B, C, and D.

rotation is generally needed to produce further unwinding by a tearing process in a direction generally following the fibril angle. In fig. 2, the areas between points 1 and 2 of micrograph C and between points 2 and 3 of micrograph D illustrate two stages of the tearing process. The original crack remains visible at point 1 in all micrographs of the series. Latewood tracheids exhibited a similar failure mechanism.

This paper discusses the concept and design of a mechanical device that will unravel a higher proportion of southern pine tracheids into ribbons than do conventional refiners. It also provides a preliminary evaluation of the concept in terms of sheet strength and pulp quality.

### Design concept

Although an exact theoretical model is confounded by thermo- and hydrodynamic effects and the anisotropic nature of fibers, an extension of the theory of dynamic torsional unwinding developed in earlier studies by the author (3) (4) seems applicable here.

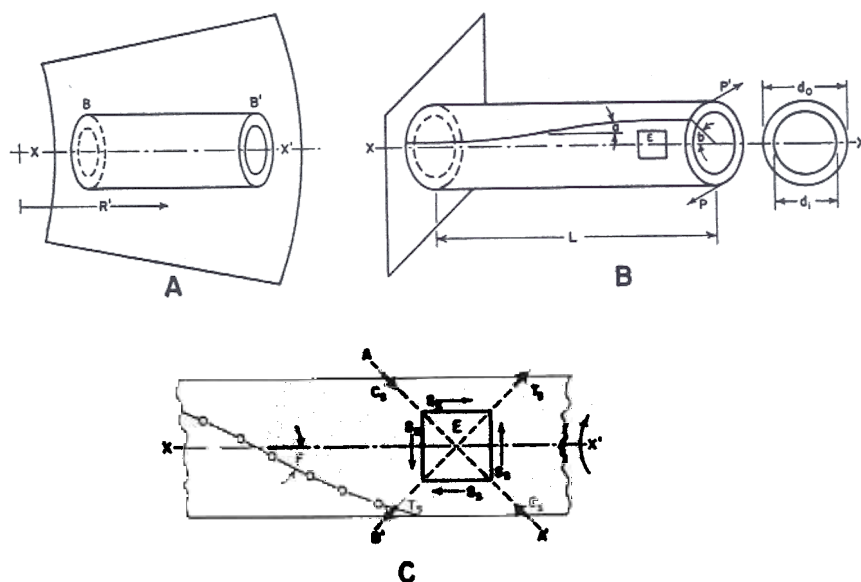
Consider a uniform, smooth-sided, right-cylindrical, intact fiber consisting of only the  $S_2$  layer and having outside diameter  $d_o$ , inside diameter  $d_i$ , and length  $L$ . Assume that during refining the longitudinal axis of the fiber becomes radially aligned (1) between the surfaces of two counterrotating disks of radius  $R$  revolving at speed  $v$  (fig. 3A). If there is no slippage, the fiber tends to rotate about its axis  $X-X'$  at a velocity proportional to the rotational velocity of the disk at distance  $R'$  from the disk center. Because the velocity of the disk varies directly with the disk radius, the rotational velocity of the fiber is slightly greater at point  $B'$  than at point  $B$ , and the fiber is acted upon by a couple of equal numerical moment but with opposite sign.

If the undeformed fiber is considered to be held in mechanical equilibrium, fig. 3B, approximates the force relationship within it. Under torsion, the shaft is twisted by a couple  $P-P'$ . The magnitude of the couple will be a function of the difference between the rotational velocities at distance  $L$  apart. Elements of the surface become helices of angle  $\alpha$ , and a radius is rotated through an angle  $b$  in length  $L$ . The state of stress of an element from the surface is pure shear (fig. 3C). Pure tension of the same magnitude as the shear stress is produced across the plane  $A-A'$  at an angle of  $45^\circ$  with the direction of the shear stress. There is an equal compressive stress on a plane  $B-B'$  at right angles to the tension plane. The stress in shear ( $S_s$ ) on the outer surface of a hollow cylinder in torsion is a function of the torsional moment ( $T$ ) and the physical dimension of the cylinder as follows:

$$S_s = 16(T) / \pi(d_o^4 - d_i^4) \quad [1]$$

As previously noted, the ribbonlike particles are formed after propagation of cracks in the direction of the  $S_2$  helix (angle  $F$ , fig. 3C). The cell wall microfibrils adhere strongly in large aggregates—termed fibrils—and

Fig. 3. Force relationships within an intact fiber during double-disk refining.



a zone of weakness exists between these aggregates. To produce the desired crack, the cell wall must be stressed beyond its strength in the zone of weakness.

For a given torsional moment, shearing stresses ( $S_r$ ) of equal magnitude are introduced parallel and perpendicular to the axis of the particle. They are accompanied by diagonal tensile ( $T_r$ ) and compressive ( $C_r$ ) stresses of equal magnitude. If the strength in shear parallel to the fiber axis or in diagonal tension is exceeded before the strength in diagonal compression, cracks may form parallel to the fibril helix and permit subsequent unwinding through visco-elastic deformations or pure rolling.

In practice, not all fibers unwind into ribbons. For example, many do not attain true radial alignment. For others which are radially aligned, the torsional moment may be insufficient to develop the required stress because of the fiber's physical dimensions, eq. [1], or inherent strength. However, if the torsional moment could be mechanically increased, the critical stresses in parallel shear and diagonal tension would be raised to higher levels—a condition favoring propagation of the initial crack and subsequent unwinding.

Consider now, a disk rotating in the clockwise direction and consisting of a series of concentric rings driven at sequentially increasing rotary speeds (fig. 4A). For example, the first ring (the ring nearest the disk center) might rotate at 500 r/min while the second might rotate at 600 r/min. Additional rings could be included with similar incremental increases in rotational speed. Since the surface velocity  $V_s$  is proportional to the rotational speed at distance  $R$  from the disk center, the velocity profile is as shown in fig. 4B. Whereas the profile of a continuous disk is a straight line, the configuration proposed here exhibits an abrupt increase in  $V_s$  at the interface between rings.

As in the previous discussion, assume that a uniform, smooth-sided, right-cylindrical, intact fiber becomes radially aligned between two opposing sets of sequential velocity rings rotating clockwise with respect to the refining surfaces. In position 1 of fig. 4A, the fiber rotates in a clockwise direction about its axis  $X-X'$  but is subjected to torsional moment and accompanying shear and tensile stresses insufficient to cause failure along the fibril helix. Hence, the fiber does not crack and no ribbon is formed.

As processing continues, the rotating fiber moves in a radial direction, eventually crossing the interface of two rings having differential velocity, as in position 2 of fig. 4A. At this point, the upper end of the fiber (the end further along the disk radius) is suddenly forced to rotate

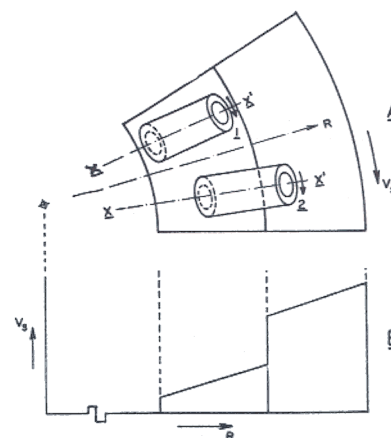


Fig. 4. A. Dynamic relationships within an intact fiber during sequential velocity refining. B. Velocity profile of refining surfaces.

in a clockwise direction at a substantially faster velocity than the lower end. The torsional moment and resulting shear and tensile stresses are immediately raised to a level sufficient to cause rupture at the fibril helix. The desired ribbon is subsequently formed by application of additional torsional stress, visco-elastic deformations, or pure rolling.

### Experimental refiner

An experimental sequential velocity refiner was designed and installed in the Forest Products Utilization Laboratory of the Southern Forest Experiment Station. The equipment is intended for laboratory-scale processing of fiber in the form of low-energy input thermomechanical or refiner mechanical pulp. Other configurations of the concept could probably be developed that would enable direct reduction of chips.

In this design, refining surfaces (comparable to the plates of a conventional double-disk refiner) are formed by the ends of two sets of four nested cylinders (fig. 5A). The outside diameters of the cylinders are 3, 4, 5, and 6 inches (ca. 75, 100, 125 and 150 mm); the wall thickness of each is 12.7 mm. Radial clearance between cylinders is about 0.08 mm. The nested cylinders are assembled within an outer housing (fig. 5B) that permits axial adjustment of the gap between the refining surfaces, and they are held in place by nuts on either end of a 50 mm hollow shaft (fig. 5C). The entire system is sealed with O-rings and can be operated at elevated air or steam pressures.

The cylinders in each set are belt-driven by separate pulleys (fig. 5D) in a clockwise direction at rotational velocities that increase from the inner to the outermost

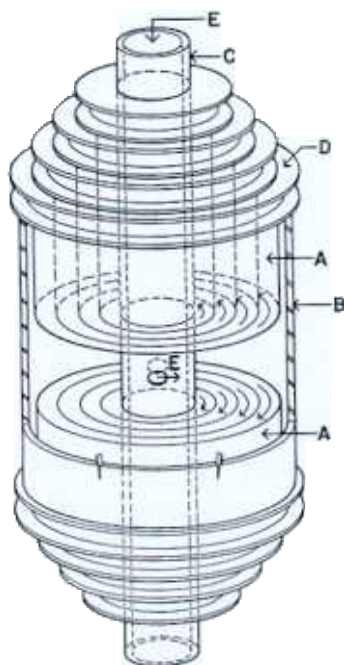


Fig. 5. Perspective view of the sequential velocity refiner.

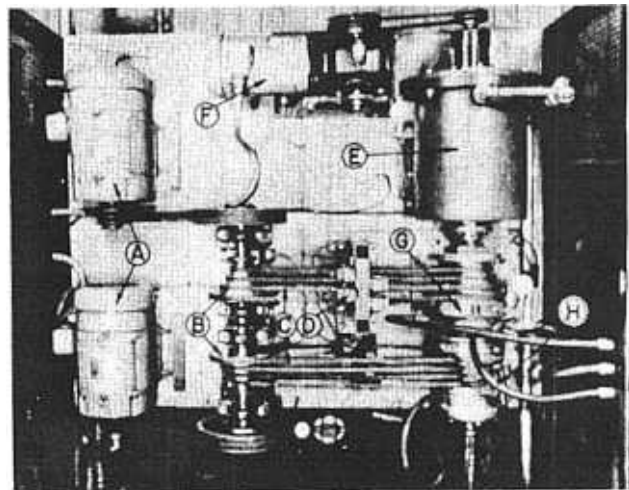


Fig. 6. General view of the experimental sequential velocity refiner.

cylinders. Velocity differentials can be varied by altering the ratio between a 4-step driving pulley and the driven pulleys attached to the cylinders. Separate variable speed, 1.5 kW, D.C. motors power each set of cylinders and provide overall speed adjustment. The unit can also serve as a conventional double-disk refiner when the individual cylinders are locked together. Fiber is fed to the refining chamber with a variable speed screw conveyor located within the hollow central shaft (fig. 5E).

Fig. 6 shows a general view of installation including drive motors (A), 4-step cone pulleys (B), pulley belts (C), idler pulleys (D), fiber steaming tank (E), feed screw drive motor (F), refiner assembly (G), and product eject lines (H). Although not visible in fig. 6, a control station and associated instrumentation are available to monitor speed, power, and temperature.

Because of the rigid, precision design used to construct the laboratory refiner and because energy inputs were low, mechanical deflection was minimal and it was possible to maintain very close clearances between individual rings and between disk surfaces. A fluted taper provided on the innermost one-third portion of the first ring in connection with a positive steam pressure differential across the refining surface, facilitated a reproducible and uniform fiber feed. The operating life of the O-ring seals was sufficient to maintain pressurization and power inputs during the course of the relatively brief experimental runs. No difficulties were experienced in operation of the main drive system.

### Evaluation procedure and results

Since the refiner was designed to process partially fiberized material, southern pine (*Pinus spp.*) pulp was obtained from the first-stage thermomechanical refiner of a commercial pulping operation. Input chips to this double-disk refiner were steamed for 2.5 minutes and fiberized at 4332 MJ/A.D.t (61 hpd/A.D.t). A small

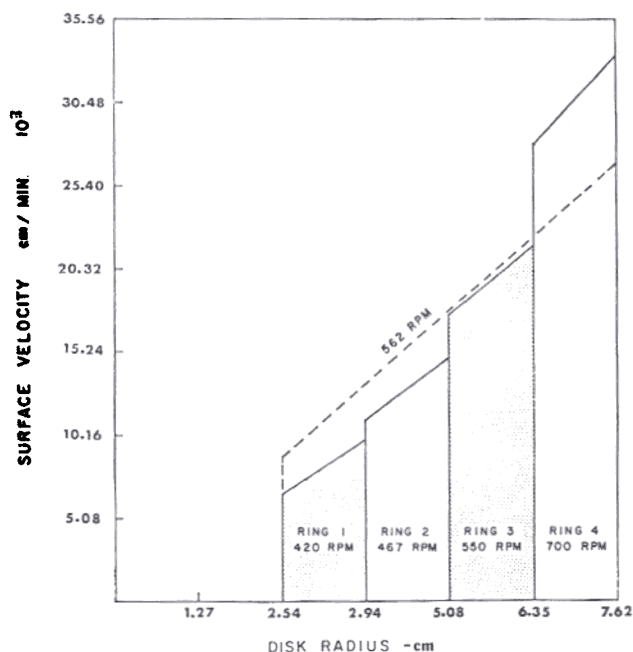


Fig. 7. Velocity profile of the refining surface when operated with sequential velocity (shaded area) and as a conventional double-disk refiner (dashed line).

amount of formaldehyde was added to the resulting fiber which was held at 4°C until used.

Some of the partially fiberized material was processed in the experimental refiner with the sequential velocity feature, and some without. For material refined with sequential velocity, rotational speeds varied from 420 r/min for ring 1 to 700 r/min for ring 4 (fig. 7); surface velocities ranged from 1.12 m/s to 5.59 m/s. The ratio of velocity increase at the interface of rings 1 and 2 was 1.11 to 1; it was 1.25 to 1 at rings 2 and 3 and 1.27 to 1 at rings 3 and 4. When the rings were locked together, a rotational speed of 562 r/min was selected because it most closely approximated the average condition attained when the unit was operated with sequential velocity.

Because a degree of roughness was deemed necessary, the refining surfaces were sandblasted to a roughness equivalent to 100 grit sandpaper. Clearance between the refining surfaces was held at  $0.13 \pm 0.05$  mm and the nominal feed rate was 13 g/min (ovendry).

Three refiner runs (replications) were made for each of the two test conditions (with and without sequential velocity). For each, about 1 kg of ovendry fiber was removed from cold storage and placed in the steaming tank. The tank and refining chamber were then steam pressurized (138 kPa); when the temperature in the tank stabilized at about 125°C, the refiner disks and feed screw were activated. A choke valve located in the product eject manifold maintained a pressure drop across the refining zone of about 70 kPa. All runs were for 15 minutes.

The refining conditions described above were derived from a number of preliminary tests; they were known to yield pulps of relatively good quality and were within operational limitations imposed by the present equipment. No attempt was made to optimize quality by selecting other operating parameters.

Shives were removed from the pulps by means of a laboratory flat-screen with 0.38 mm slots. Handsheets were made from each pulp at nominal grammages of 60, 70, 80, and 90 g/m<sup>2</sup> in accordance with the TAPPI standard method. Sheets were made directly from the refined pulp since preliminary tests indicated treatment for removal of latency yielded erratic results. Five sheet properties were determined: grammage, density, burst factor, tear factor, and breaking length. Pulp properties measured included Canadian standard freeness, *S* (in terms of the 48/100 fraction CSF) and *L*, and the standard Bauer screen classification. (In this connection *S* and *L* denote fiber qualities according to Forgas.)

In addition, some of the partially fiberized raw material from the thermomechanical refiner was screened, made into handsheets, and tested. Because of their expected low strength, sheets were made at nominal grammages of 70, 80, and 90 g/m<sup>2</sup>. Pulp quality was also determined.

Sheets made from both laboratory pulps were denser and stronger than sheets made from the raw fiber (table 1). Sheet density was higher and burst factor and breaking length were greater for fiber refined with sequential velocity than for fiber refined without it. By the t-test for unpaired data, these means proved significantly different at the 0.05 level. There was no significant difference between the means observed for tear factor (av. 79.9) or grammage (av. 78.3).

Pulp properties reflect the higher strengths observed for sheets made from sequential velocity pulp (table 1). Canadian standard freeness of the raw fiber was 672 ml

Table 1. Handsheet properties and pulp characteristics of raw fiber and pulp made with and without sequential velocity

Property	Raw fiber	Without seq. vel. <sup>1</sup>	With seq. vel. <sup>1</sup>
Grammage, g/m <sup>2</sup>	81.7	80.2	76.4
Density, g/cm <sup>3</sup>	0.238	0.308	0.334
Burst factor	3.7	10.1	12.4
Tear factor	58.6	80.5	79.2
Breaking length, m	1005	2164	2580
Canadian standard freeness, ml	672	307	172
<i>S</i> -factor, ml	724	673	642
<i>L</i> -factor, %	68.9	59.7	52.3
Bauer screen classification, %			
R28	46.3	36.1	28.2
28/48	22.6	23.6	24.0
48/100	6.1	7.3	8.5
100/200	3.4	5.4	6.1
P200	21.6	27.6	33.2

<sup>1</sup> Values are means of the three refiner replications

**Table 2. Sheet properties for raw fiber and for pulp produced with and without sequential velocity.**

Property	Raw fiber	Without seq. vel.	With seq. vel.
Sheet density, g/cm <sup>3</sup>	0.226		
Burst factor	2.8		
Tear factor	50.2		
Breaking length, m	932.0		

but was reduced to 172 ml for sequential velocity pulp as compared to 307 ml when sequential velocity was not used. The values obtained for the *L*-factor and the Bauer screen classification reveal a slightly greater reduction of the long fiber fraction for pulps made with sequential velocity than for those made without it. The *S* value was least for sequential velocity pulp, indicating an increase in specific surface. Probably, a proportion of the increase in specific surface can be attributed to greater numbers of unwound tracheids.

Linear regression analysis of the relationship between grammage and a given sheet property yielded equations of good fit for pulps made with and without sequential velocity and for the raw fiber. For each property, the slope of the relationship was essentially the same for the three types. With these equations, sheet properties were calculated at the more commonly reported grammage of 60 g/m<sup>2</sup> as shown in *table 2*.

When the properties of the raw fiber are compared to those obtained for sequential velocity pulp, the increases for sheet density, burst, tear, and breaking length were 28.6, 296.4, 46.2, and 166.1%, respectively. When sequential velocity was not used, the values were 17.7, 214.3, 49.6, and 121.0%.

The Bauer screen fractions (R28, 28/48, 48/100, and 100/200) of the raw fiber and pulps made with and without sequential velocity were also examined in a light microscope to provide a visual assessment of fiber characteristics. Four types (intact, frazzled, broomed, and ribbon-strand) were readily identified. Little debris was present in these fractions and was not considered.

Intact fibers (*fig. 8A*) were generally well isolated, of varying length, with little or no external cell wall fibrillation. Frazzled fibers (*fig. 8B*) were similar to intact fibers except that external fibrillation of the primary and secondary wall was clearly evident. Broomed fibers (*fig. 8C*) exhibited fibrillation or unwinding into ribbon- or strand-like material on one or both ends of a generally intact fiber. A well defined ribbon is illustrated in *fig. 1*. Strand material appeared to be derived from broken portions of ribbons and was included in the ribbon group.

Dilute slurries of the fiber fractions from each of two machine replications were examined. The microscope stage was systematically traversed and all fibers passing within the field of view were classified into the types described above. One hundred observations were made for each sample. The averaged results, expressed as a number percentage, are given in *table 3*. Differences between means were tested by variance analysis at the 0.05 level.

For the R28 fraction, the proportion of intact fibers was reduced by both refining methods but was less (av. 61.00%) when sequential velocity was used than when it was not (av. 71.33%). While the number of frazzled fibers increased for both refining techniques, there were more frazzled fibers when sequential velocity was used (av. 20.33%) than when it was not (av. 13.34%). The

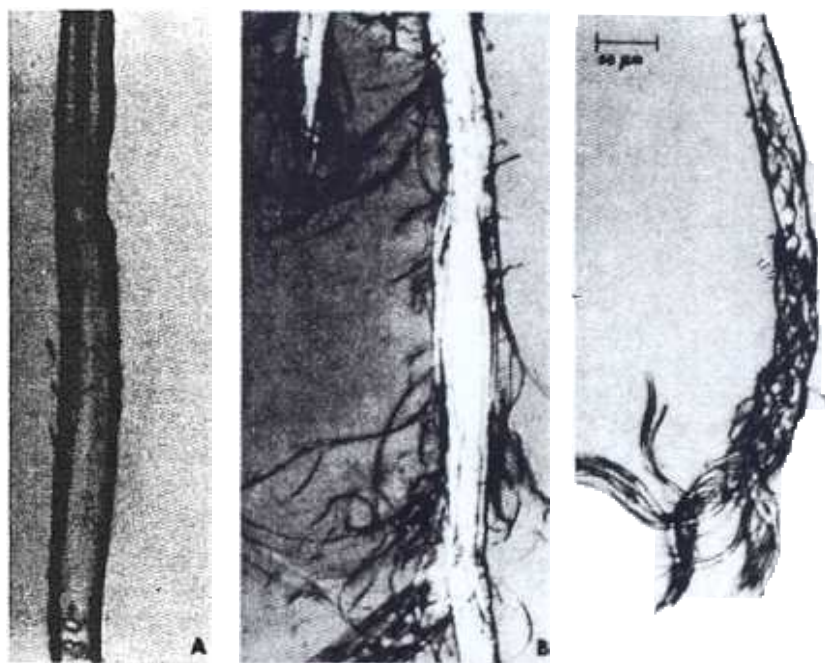


**Fig. 8. Fiber types identified in refined pulp.**

- A. Intact
- B. Frazzled
- C. Fibrillated.

C The scale mark in C is also applicable to A and B.

**Table 3. Number percentage of fiber types in Bauer screen fractions for raw fiber and pulps made with and without sequential velocity.**

Types of fibers examined Classification, %	Bauer fraction											
	R28			28/48			48/100			100/200		
	Raw fiber	Without seq. vel.	With seq. vel.	Raw fiber	Without seq. vel.	With seq. vel.	Raw fiber	Without seq. vel.	With seq. vel.	Raw fiber	Without seq. vel.	With seq. vel.
Intact	81.00	71.33	61.00	77.17	58.33	43.66	58.67	51.67	29.66	26.33	21.00	11.83
Frazzled	8.50	13.34	20.33	4.50	13.67	19.67	2.50	7.16	9.84	0.00	2.83	2.17
Broomed	9.00	10.50	14.33	11.17	16.67	22.67	14.00	17.67	18.33	5.50	6.50	5.33
Ribbon-strand	1.50	4.83	4.34	7.16	11.33	14.00	24.83	23.50	42.17	68.17	69.67	80.67

proportion of broomed fibers was unaffected when the raw fiber was refined without sequential velocity (av. 9.75%) but increased to 14.33% when sequential velocity was used. There was no significant difference between means for ribbon-strand particles (av. 3.56%).

The 28/48 fraction exhibited a similar trend. The proportion of intact fibers was less and the percentage of frazzled and broomed fibers was greater for raw fiber refined with sequential velocity than when refined without sequential velocity. The proportion of ribbons and strands was unaffected by the refining method (av. 12.67%).

The 48/100 fraction is of particular interest because it was used for determination of "S" values. For this fraction, the proportion of intact fibers was substantially less when raw fiber was refined with sequential velocity (av. 29.66%) than when it was refined without sequential velocity (av. 51.68%). The percentage of frazzled and broomed fibers was unaffected by the refining method (av. 8.50% and 18.00%, respectively). The proportion of ribbons and strands did not differ from the raw fiber when refined without sequential velocity (av. 24.17%) but increased when sequential velocity was used (av. 42.17%). Thus, refining with sequential velocity produced a pulp fraction containing a substantially lower proportion of intact fibers and greater numbers of ribbons and strands than when refining without sequential velocity; the proportion of frazzled and broomed fibers was unaffected by the refining method. This result would be expected to yield a fraction of higher specific surface and is in agreement with the trends observed for "S" values.

The 100/200 fraction exhibited the same trends as the 48/100 fraction. Fiber refined with sequential velocity produced a pulp containing a lower proportion of intact fibers and greater numbers of ribbons and strands than when refining without sequential velocity while the proportion of frazzled and broomed fibers was unaffected by the refining method.

Specific energy consumption is an important process parameter and of increasing practical concern. While it was possible to monitor total motor effect demand during refining, the no-load idling loss was not constant due to entrapment of small quantities of fiber between disk segments and within O-ring seals. Thus, power

measurements made during the experiment proved of limited value.

In a series of subsequent runs, power levels were intermittently sampled by feeding fiber to the refiner for 15 seconds at a rate of 13 g/min followed by a 15-second period of no-load operation. The procedure was repeated 20 times in each of three replications. All other conditions were as in the principal experiment. The mean loads for each condition were averaged; the difference between total-load and no-load power was taken as net energy consumed. For such non-steady state operation, specific energy demand was 589 MJ/A.D.t when refining without sequential velocity and 724 MJ/A.D.t when operating with sequential velocity. There was no significant difference between the means (av. 660 MJ/A.D.t) at the 0.05 level. This result suggests that sequential velocity refining may offer an important energy advantage over conventional double-disk refining since sequential velocity pulps were refined to a much lower freeness at the same level of energy input.

### Discussion

The purpose of this experiment was to evaluate a machine design concept based on the author's theory of dynamic torsional unwinding as a means to effectively increase the specific surface of pulps made by mechanical means. The results appear to justify the approach in terms of three measures—handsheet strength was improved, pulp quality was enhanced, and the number of particles having increased specific surface was greater when the refiner was operated with sequential velocity than when it was operated as a conventional double-disk refiner.

It is difficult to project the properties of sequential velocity pulps made with a small laboratory device to those one might obtain with a refiner of greater capability. For example, increasing the number of rings should improve the probability of fiber unwinding and hence yield sheets of higher strength. This can be illustrated with the present refiner by reprocessing first-pass pulps in a second-pass. In a series of subsequent experiments, the proportion change in properties between one- and two-pass refining was noted and applied to the values obtained for sheets made at 60 g/m<sup>2</sup> in the main experi-

ment. Results from the second pass, projected from first pass data, are tabulated below:

Density g/cm <sup>3</sup>	0.365
Burst factor	15.4
Tear factor	80.4
Breaking length, m	3,076
Freeness, ml	120
S, ml	602
L, %	50.4

Assuming an additional 660 MJ/A.D.t was applied in second-stage sequential velocity refining, the total energy expended was about 5659 MJ/A.D.t. The values tabulated compare favorably with those from commercial 3-stage thermomechanical pulps of southern pine requiring in excess of 8521 MJ/A.D.t.

#### Acknowledgment

The author acknowledges the cooperation and assistance of Dr. R. W. Strauss and Mr. B. Z. Workmen of Bowater, Inc.

#### Literature

1. *Atack, D. and May, W. D.*: High speed photography of particle motion in a disc refiner. In Proc. 9th Int. Congr. High-speed Photography (1970). Soc. Motion Picture and Television Engr. N.Y. 2 p.
2. *Forgacs, O. L.*: The characterization of mechanical pulps. Pulp Pap. Mag. Can. 64 (1963) T89.
3. *McMillin, C. W.*: Aspects of fiber morphology affecting properties of handsheet made from loblolly pine refiner groundwood. Wood Sci. Technol. 3 (1969) 139.
4. *McMillin, C. W.*: Dynamic torsional unwinding of southern pine tracheids as observed in the scanning electron microscope. Svensk Papperstidn. 77 (1974): 9, 319.

(First manuscript received November 29, 1977.

Revised October, 1978)

Reprinted from: SVENSK PAPPERSTIDNING NO. 18-1978: 567-574.